

A Semi-analytic Formulation for Relativistic Blast Waves with a Long-lived Reverse Shock

Z. Lucas Uhm^{1,2}

*Institute for the Early Universe and Research Center of MEMS Space Telescope,
Ewha Womans University, Seoul 120-750, South Korea*

and

Institut d'Astrophysique de Paris, 98 bis boulevard Arago, 75014 Paris, France

ABSTRACT

This paper performs a semi-analytic study of relativistic blast waves in the context of gamma-ray bursts (GRBs). Although commonly used in a wide range of analytical and numerical studies, the equation of state (EOS) with a constant adiabatic index is a poor approximation for relativistic hydrodynamics. Adopting a more realistic EOS with a variable adiabatic index, we present a simple form of jump conditions for relativistic hydrodynamical shocks. Then we describe in detail our technique of modeling a very general class of GRB blast waves with a long-lived reverse shock. Our technique admits an arbitrary radial stratification of the ejecta and ambient medium. We use two different methods to find dynamics of the blast wave: (1) customary pressure balance across the blast wave and (2) the “mechanical model”. Using a simple example model, we demonstrate that the two methods yield significantly different dynamical evolutions of the blast wave. We show that the pressure balance does not satisfy the energy conservation for an adiabatic blast wave while the mechanical model does. We also compare two sets of afterglow light-curves obtained with the two different methods.

Subject headings: gamma-ray burst: general — hydrodynamics — shock waves

¹E-mail: uhm@iap.fr

²International Center for Astrophysics, Korea Astronomy and Space Science Institute, Daejeon 305-348, South Korea

1. Introduction

The afterglow emission of a gamma-ray burst (GRB) is believed to be produced by a relativistic blast wave (Mészáros & Rees 1997). The relativistic blast wave is driven by an “ejecta”, which is ejected by the central engine of the GRB explosion. As the ejecta interacts with a surrounding ambient medium, two (forward and reverse) shock waves develop (e.g., Piran 2004). The forward shock (FS) wave sweeps up the ambient medium, and the reverse shock (RS) wave propagates through the ejecta.

As the blast wave has high Lorentz factors $10^2 - 10^3$ (e.g., Mészáros 2006), the FS wave is highly relativistic and an equation of state (EOS) with a constant adiabatic index $4/3$ may well describe the gas in the FS-shocked region. However, the strength of the RS wave varies as the blast wave propagates. In the case of a constant-density ambient medium, the RS wave is initially non-relativistic and then transitions to a mildly-relativistic or relativistic regime (Kobayashi 2000; Sari & Piran 1995). Thus, an EOS with a constant adiabatic index is not adequate for the gas in the RS-shocked region; a variable adiabatic index needs to be considered to account for change in the gas temperature.

Although the EOS with a constant adiabatic index has been widely used in analytical and numerical studies of relativistic hydrodynamics, it is valid only for the gas of either non-relativistic (with the index $5/3$) or ultra-relativistic temperature (with the index $4/3$). The correct EOS for a relativistic ideal gas is formulated in terms of modified Bessel functions (e.g., Synge 1957), and its equivalent adiabatic index varies from $5/3$ to $4/3$ as the temperature increases.

As it is not convenient to deal with modified Bessel functions, there has been effort to find simpler EOSs that closely reproduce the correct EOS of a relativistic ideal gas. Taub (1948) showed that the choice of EOS is not arbitrary and must satisfy a certain inequality (Taub’s inequality). By taking the equal sign in Taub’s inequality, Mignone et al. (2005) derived a simple form of EOS that has correct limiting values $5/3$ and $4/3$.

The same EOS as in Mignone et al. (2005) was previously introduced by Mathews (1971), considering a relativistic “monoenergetic” gas where all particles have the same energy. The validity of this EOS was addressed by Blumenthal & Mathews (1976) for the cases of both infinite mean free collision times and very short mean free collision times. This EOS was also adopted by Meliani et al. (2004) and Mignone & McKinney (2007). In particular, Mignone & McKinney (2007) demonstrated in their relativistic numerical simulations that use of an EOS with a constant adiabatic index can significantly endanger the solution when transitions from cold to hot gas (or vice versa) are present.

We use the same above EOS in this paper. Following Mathews (1971), we consider

a relativistic monoenergetic gas and show that it closely reproduces the correct EOS of a relativistic ideal gas. Then we use this EOS to find a simple form of jump conditions for relativistic hydrodynamical shocks. This simple set of jump conditions applies to shocks of arbitrary strength.

A short-lived RS was proposed to explain a brief optical flash (Mészáros & Rees 1999; Sari & Piran 1999a, 1999b). A dynamical evolution of such a short-lived RS was studied analytically by assuming an equality of pressure across the blast wave (Kobayashi 2000; Sari & Piran 1995). The RS wave here is short-lived since the ejecta is assumed to have a constant Lorentz factor. However, in general, the ejecta is expected to emerge with a range of the Lorentz factors. The shells with lower Lorentz factors will gradually “catch up” with the blast wave as it decelerates. Thus, the RS wave is long-lived. Such a long-lived RS was studied for a power-law ejecta by assuming a constant ratio of the two pressures at the FS and RS (Rees & Mészáros 1998).

In this paper, we present a detailed description of our blast-wave modeling technique for even more general class of explosions where the ejecta and the ambient medium have an arbitrary radial structure or stratification. More specifically, we study analytically the spherical expansion of such a stratified ejecta, and find the trajectory of the RS wave through the ejecta self-consistently. In order to find a dynamical evolution of the blast wave, we use two different methods: (1) customary pressure balance and (2) the “mechanical model” (Beloborodov & Uhm 2006).

Using a simple example model, we demonstrate that, although the customary assumption of pressure balance for the blast wave yields an estimated evolution, it is not rigorously accurate. In particular, the energy conservation is not satisfied for an adiabatic blast wave; the total energy is decreased by a factor of 5 in the case of the example model.

The mechanical model was developed for relativistic blast waves, by relaxing the pressure balance (or proportionality) and applying the conservation laws of energy-momentum tensor and mass flux on the blast between the FS and RS. Using the same example model, we show that the energy conservation is satisfied for the mechanical model. We also show that dynamical evolutions found by the two methods differ significantly. Finally, we present the afterglow light-curves in X-ray and optical bands. We compare two sets of light-curves corresponding to the two different dynamical evolutions mentioned above.

In Section 2, we derive a simple set of jump conditions for relativistic hydrodynamical shocks. In Section 3, we describe in detail our blast-wave modeling technique. We also provide a simple method of evaluating the blast energy, employing a Lagrangian description for the blast wave. In Section 4, we review the mechanical model including more detailed

equations.

2. Relativistic shocks

We consider a shock wave of an arbitrary strength. The preshock medium (cold) is denoted by region 1, and the postshock medium (hot) by region 2. The gas moves at right angles to the surface of discontinuity (shock front). The rest-mass density ρ , the energy density e (including rest energy), and the pressure p of the gas are defined in the rest frame of each region. The energy-momentum tensor $T^{\alpha\beta}$ for a perfect fluid and the mass flux j^α are given as

$$T^{\alpha\beta} = (e + p)u^\alpha u^\beta + g^{\alpha\beta}p, \quad \text{and} \quad j^\alpha = \rho u^\alpha, \quad (1)$$

where $g^{\alpha\beta}$ is the Minkowski metric, and u^α is the 4-velocity of the gas.

2.1. Jump conditions

A shock is described by three jump conditions that express the continuity of mass, energy, and momentum flux densities, respectively, in the shock frame (Landau & Lifshitz 1959),

$$\gamma_2 \beta_2 \rho_2 = \gamma_1 \beta_1 \rho_1, \quad (2)$$

$$\gamma_2^2 \beta_2 (e_2 + p_2) = \gamma_1^2 \beta_1 \rho_1 c^2, \quad (3)$$

$$\gamma_2^2 \beta_2^2 (e_2 + p_2) + p_2 = \gamma_1^2 \beta_1^2 \rho_1 c^2. \quad (4)$$

Here subscripts 1 and 2 refer to regions 1 and 2, and c is the speed of light. The Lorentz factor γ of the gas for each region is measured in the rest frame of shock front, and thus $\beta = (1 - 1/\gamma^2)^{1/2}$ is the gas velocity relative to the shock front. Notice that we have set $p_1 = 0$ and $e_1 = \rho_1 c^2$ here since we assume that region 1 is cold.

We introduce a quantity κ in writing an equation of state for the relativistic gas in region 2,

$$p_2 = \kappa_2 (e_2 - \rho_2 c^2). \quad (5)$$

We use the quantity κ instead of an adiabatic index, in order to avoid any confusion with the Lorentz factors. Note that κ_2 is 2/3 for a non-relativistic shocked gas, and 1/3 for an ultra-relativistic gas. As mentioned in Section 1, we do not use a constant value for κ_2 . The quantity κ_2 here varies between 1/3 and 2/3 as the strength of the shock varies.

We solve these 4 equations (2)-(5) algebraically. First, we define a compression ratio $a \equiv \rho_2/\rho_1$ and get the relation $\gamma_1^2 = a^2(\gamma_2^2 - 1) + 1$ by squaring the equation (2). Then, substituting γ_1^2 and e_2 (from the equation [5]) into the equations (3) and (4), we find the expressions for γ_1, γ_2 , and p_2 in terms of κ_2 and the compression ratio a ,

$$\gamma_2^2 = \frac{(a+1)}{a(1-\kappa_2^2) + (1+\kappa_2)^2}, \quad \gamma_1^2 = \frac{(a+1)[a\kappa_2 - (1+\kappa_2)]^2}{a(1-\kappa_2^2) + (1+\kappa_2)^2}, \quad (6)$$

$$p_2/(\rho_1 c^2) = \frac{(a\kappa_2)^2 - (a\kappa_2)(2+\kappa_2)}{(1+\kappa_2)}, \quad (7)$$

where we have used the fact that $a(1-\kappa_2) + (1+\kappa_2)$ can not be zero for $a > 0$ and $1/3 \leq \kappa_2 \leq 2/3$. The equations (6) and (7) are exact.

The shock strength may be described by the relative velocity $\beta_{12} = (\beta_1 - \beta_2)/(1 - \beta_1\beta_2)$, or by the relative Lorentz factor $\gamma_{12} = (1 - \beta_{12}^2)^{-1/2}$, which is given by

$$\gamma_{12} = (1 - \beta_1\beta_2)\gamma_1\gamma_2 = \gamma_1\gamma_2 - [(\gamma_1^2 - 1)(\gamma_2^2 - 1)]^{1/2}. \quad (8)$$

The shock strength γ_{12} is then directly calculated using the equation (6),

$$\gamma_{12} = \frac{(a\kappa_2 - 1)}{(1 + \kappa_2)}. \quad (9)$$

Thus, we find a very simple form for the compression ratio a in terms of κ_2 and γ_{12} ,

$$a = \frac{\rho_2}{\rho_1} = \frac{(1 + \kappa_2)\gamma_{12} + 1}{\kappa_2}. \quad (10)$$

Substituting the compression ratio (10) into the equations (6) and (7), we now express γ_1, γ_2 , and p_2 in terms of κ_2 and γ_{12} ,

$$\gamma_1^2 = \frac{(\gamma_{12} + 1)[(1 + \kappa_2)\gamma_{12} - \kappa_2]^2}{(1 - \kappa_2^2)\gamma_{12} + (1 + \kappa_2^2)}, \quad (11)$$

$$\gamma_2^2 = \frac{(\gamma_{12} + 1)}{(1 - \kappa_2^2)\gamma_{12} + (1 + \kappa_2^2)}, \quad (12)$$

$$p_2 = (\gamma_{12} - 1)[(1 + \kappa_2)\gamma_{12} + 1] \rho_1 c^2. \quad (13)$$

As we shall see below, κ_2 here is in fact a function of γ_{12} , and therefore the shock strength γ_{12} becomes the only free parameter of the shock. Combining equations (5), (10), and (13), we verify an expected relation,

$$e_2 = \frac{1}{\kappa_2} p_2 + \rho_2 c^2 = \gamma_{12} \rho_2 c^2, \quad (14)$$

which means that the shock strength γ_{12} is equal to the mean random Lorentz factor of particles in the postshock medium (measured in its fluid frame).

It may be noticed that there are only three independent equations among (10) to (14), since we had three jump conditions in the beginning. In fact, three of them are equivalent to those equations that appear on Blandford & McKee (1976).

2.2. Relation between κ and mean Lorentz factor $\bar{\gamma}$

2.2.1. Relativistic ideal gas

We briefly review a relativistic ideal gas where a particle of mass m and momentum \tilde{p} has the energy $\epsilon(\tilde{p}) = mc^2 [1 + (\tilde{p}/mc)^2]^{1/2}$. The Maxwellian momentum distribution function $f(\tilde{p})$ is given as $f(\tilde{p}) = A \tilde{p}^2 \exp[-\epsilon(\tilde{p})/(k_B T)]$, where A is a proportionality constant, k_B is the Boltzmann constant, and T is the temperature of the gas. Using a normalization condition on the number density, $n = \int_0^\infty f(\tilde{p}) d\tilde{p}$, the proportionality constant is found to be $A = \frac{n}{(mc)^3} \frac{u}{K_2(u)}$, with a modified Bessel function K_2 . Here we have defined $u \equiv (mc^2)/(k_B T)$, which basically measures how relativistic the gas is; $u \gg 1$ corresponds to a non-relativistic limit, and $u \ll 1$ to an ultra-relativistic limit. We evaluate the integrals of pressure and energy density of the gas:

$$p = \frac{1}{3} \int_0^\infty \tilde{p} v(\tilde{p}) f(\tilde{p}) d\tilde{p} = nk_B T, \quad (15)$$

$$e = \int_0^\infty \epsilon(\tilde{p}) f(\tilde{p}) d\tilde{p} = (n mc^2) \left(\frac{K_1(u)}{K_2(u)} + \frac{3}{u} \right), \quad (16)$$

where $v(\tilde{p})$ is the velocity of a particle of momentum \tilde{p} , and $K_1(u)$ is also a modified Bessel function. See Greiner, Neise, & Stocker (1995) for an alternative derivation. The equation (16) gives the mean Lorentz factor $\bar{\gamma}$ of particles as

$$\bar{\gamma} = \frac{K_1(u)}{K_2(u)} + \frac{3}{u}. \quad (17)$$

The quantity κ (defined in the equation [5]) is given as

$$\kappa_i = \frac{p}{e - \rho c^2} = \left[u \left(\frac{K_1(u)}{K_2(u)} + \frac{3}{u} - 1 \right) \right]^{-1}. \quad (18)$$

Here the subscript i refers to a relativistic *ideal* Maxwellian gas. Since both $\bar{\gamma}$ and κ_i are given in terms of u only, one should be in principle able to express κ_i as a function of $\bar{\gamma}$. However, it is not easy to do so analytically, as it involves two modified Bessel functions K_1 and K_2 . This becomes a good motivation of considering the following monoenergetic gas.

2.2.2. Monoenergetic gas

Here we consider a “monoenergetic” gas, where all particles in the gas have the same momentum \bar{p} (or the same Lorentz factor $\bar{\gamma}$) (e.g., Mathews 1971). We show below that the behavior of this gas is very close to that of a relativistic ideal gas. The momentum distribution function is simply given by a Dirac-delta function, $f(\tilde{p}) = n \delta(\tilde{p} - \bar{p})$, which satisfies the normalization condition, $n = \int_0^\infty f(\tilde{p}) d\tilde{p}$. We evaluate the integrals of pressure and energy density for this gas:

$$p = n (mc^2) \frac{\bar{\gamma}^2 - 1}{3\bar{\gamma}}, \quad e = n (\bar{\gamma} mc^2). \quad (19)$$

Therefore, the corresponding κ is found to be

$$\kappa_m = \frac{p}{e - \rho c^2} = \frac{1}{3} \left(1 + \frac{1}{\bar{\gamma}} \right), \quad (20)$$

where the subscript m refers to a *monoenergetic* gas. Note that κ_m has the correct limiting value $2/3$ for a non-relativistic gas, and $1/3$ for an ultra-relativistic gas. We compare this monoenergetic gas with a relativistic ideal gas, by computing κ_m/κ_i numerically as a function of $\bar{\gamma}$. The result is shown in Figure 1. Notice that there is only 4.8 % of maximal difference at about $\bar{\gamma} = 1.6$, and two gases are practically identical especially for high Lorentz factors above 10.

The relation (20) is simple, and thus very useful in dealing with a relativistic gas. In the following section, we show that the jump conditions (10)-(14) simplify significantly when the gas is treated as monoenergetic.

2.3. Jump conditions of a monoenergetic gas

We continue on the problem of a relativistic shock wave for the case of a monoenergetic gas. When the gas in the postshock medium (region 2) is treated as monoenergetic, the quantity κ_2 satisfies

$$\kappa_2 = \frac{1}{3} \left(1 + \frac{1}{\gamma_{12}} \right), \quad (21)$$

since the mean Lorentz factor in the equation (20) is equal to the shock strength γ_{12} as shown in the equation (14). Using the relation (21), we re-write the jump conditions (10)-(14) in terms of γ_{12} only:

$$\gamma_1^2 = \frac{(4\gamma_{12}^2 - 1)^2}{8\gamma_{12}^2 + 1} \quad \text{or} \quad \beta_1 = \frac{4\beta_{12}}{\beta_{12}^2 + 3}, \quad (22)$$

$$\gamma_2^2 = \frac{9\gamma_{12}^2}{8\gamma_{12}^2 + 1} \quad \text{or} \quad \beta_2 = \frac{\beta_{12}}{3}, \quad (23)$$

$$p_2 = \frac{4}{3}(\gamma_{12}^2 - 1)\rho_1 c^2, \quad (24)$$

$$a = \rho_2/\rho_1 = 4\gamma_{12}, \quad e_2 = 4\gamma_{12}^2 \rho_1 c^2. \quad (25)$$

It has become clear that the shock strength γ_{12} is the only free parameter of the shock. We emphasize that these simple equations (22)-(25) are exact for a monoenergetic gas, and apply to shocks of arbitrary strength (relativistic, mildly-relativistic, or non-relativistic). This result is also briefly described in Beloborodov & Uhm (2006).

3. Blast waves

A central explosion of a gamma-ray burst (GRB) ejects a large amount of material with high Lorentz factors $\Gamma_{\text{ej}} \sim 10^2 - 10^3$. This ejected flow is called the “ejecta”. The ejecta expands and drives a forward shock (FS) wave into the external ambient medium. When the ejecta interacts with the ambient medium, another shock wave – a reverse shock (RS) – develops and propagates back through the ejecta. Thus this standard picture has four regions: (1) external ambient medium, (2) shocked external medium, (3) shocked ejecta, and (4) unshocked ejecta (e.g., Piran 2004). In Figure 2, we show schematically these 4 regions. The shocked external medium is separated from the shocked ejecta by a contact discontinuity (CD). Two shocked regions 2 and 3 between the FS and RS are hot and called the “blast”.

We assume that the whole blast moves with a common Lorentz factor Γ . This is reasonable since internal motions in the blast are subsonic, and hydrodynamical simulations confirm that $\Gamma \approx \text{const}$ between the FS and RS (Kobayashi & Sari 2000). The Lorentz factors Γ_f , Γ_r and Γ_{ej} , denoting for the FS, RS, and ejecta respectively, are measured in the lab. frame. The ambient medium is at rest in the lab. frame. The rest-mass density ρ , energy density e (including rest energy), and pressure p in each region are measured in its own rest frame. It is assumed that the ambient medium and ejecta are ‘cold’, having no pressure.

3.1. Radially stratified ejecta

The explosion ejecta is viewed as a sequence of shells that coast with Lorentz factors Γ_{ej} . Each shell is prescribed an ejection time τ . The ejection time plays the role of Lagrangian

coordinate that labels the shells in the ejecta. Theoretically, the ejecta is expected to emerge with a monotonic velocity profile as a result of internal shocks that take place at small radii $r < 10^{16}$ cm (e.g., Piran 2004). At the end of the internal-shock stage, any two adjacent shells no longer collide with each other. Thus we consider here only a non-increasing function of $\Gamma_{\text{ej}}(\tau)$; $\Gamma'_{\text{ej}}(\tau) \equiv d\Gamma_{\text{ej}}/d\tau \leq 0$. Notice that Γ_{ej} should remain independent of the lab. time t as each shell coasts without colliding with another shell. The corresponding velocity $v_{\text{ej}}(\tau) = c(1 - 1/\Gamma_{\text{ej}}^2)^{1/2}$ is also non-increasing. The initial density of the ejecta may, however, have an arbitrary radial profile. The evolution of such “stratified” ejecta is analytically studied here, restricted to the unshocked ejecta.

We assume spherical symmetry. However, the calculation remains valid even if the explosion is driven by a jet with a small opening angle θ_{jet} as long as $\Gamma_{\text{ej}} \gg \theta_{\text{jet}}^{-1}$; the jet behaves like a portion of spherical ejecta since the edge of the jet is causally disconnected from its axis.

3.1.1. Continuity equation of stratified ejecta

The 4-velocity u^α for a spherically symmetric ejecta is written in spherical polar coordinates (ct, r, θ, ϕ) as $u^\alpha = \Gamma_{\text{ej}}(c, v_{\text{ej}}, 0, 0)$, where t indicates the lab. time, and r is the radius measured from the center of the explosion. The continuity equation for ejecta is simply $\nabla_\alpha(\rho_{\text{ej}}u^\alpha) = 0$. Here the ejecta density ρ_{ej} is measured in the rest frame of ejecta. Then the continuity equation reads

$$\frac{1}{c} \frac{\partial}{\partial t} \bigg|_r (\rho_{\text{ej}} \Gamma_{\text{ej}} c) + \frac{1}{r^2} \frac{\partial}{\partial r} \bigg|_t (r^2 \rho_{\text{ej}} \Gamma_{\text{ej}} v_{\text{ej}}) = 0, \quad (26)$$

which becomes

$$\frac{\partial}{\partial t} \bigg|_r (\rho_{\text{ej}} \Gamma_{\text{ej}}) + \frac{\partial}{\partial r} \bigg|_t (\rho_{\text{ej}} \Gamma_{\text{ej}} v_{\text{ej}}) + \frac{2}{r} (\rho_{\text{ej}} \Gamma_{\text{ej}} v_{\text{ej}}) = 0. \quad (27)$$

We describe below a simple way of solving the equation (27) that makes use of the Lagrangian coordinate τ .

Consider a shell in ejecta that was ejected at time τ with velocity $v_{\text{ej}}(\tau)$. The radius r of this τ -shell at time t is given by

$$r(\tau, t) = \int_\tau^t v_{\text{ej}}(\tau) dt = v_{\text{ej}}(\tau) (t - \tau). \quad (28)$$

The equation (28) is viewed as a relationship among three coordinates r , t , and τ . Any two of those can be regarded as two independent variables. In the equation (27), the coordinates

r and t are two independent variables. Since $\Gamma_{\text{ej}}(\tau)$ and $v_{\text{ej}}(\tau)$ are functions of τ only, it is useful to have τ as one of the variables instead of, e.g., time t . Using the relation (28), we eliminate time t from the equation (27), and adopt the coordinates τ and r as two independent variables. First, we partially differentiate the relation $r = v_{\text{ej}}(\tau)(t - \tau)$ with respect to t at fixed r ,

$$\left. \frac{\partial r}{\partial t} \right|_r = 0 = v'_{\text{ej}}(\tau) \left. \frac{\partial \tau}{\partial t} \right|_r \frac{r}{v_{\text{ej}}(\tau)} + v_{\text{ej}}(\tau) \left(1 - \left. \frac{\partial \tau}{\partial t} \right|_r \right), \quad (29)$$

which yields

$$\left. \frac{\partial \tau}{\partial t} \right|_r = \frac{1}{1 - r(v'_{\text{ej}}/v_{\text{ej}}^2)}, \quad (30)$$

where $v'_{\text{ej}}(\tau) \equiv dv_{\text{ej}}/d\tau$. Similarly, we differentiate the equation (28) with respect to r at fixed t ,

$$\left. \frac{\partial r}{\partial r} \right|_t = 1 = v'_{\text{ej}}(\tau) \left. \frac{\partial \tau}{\partial r} \right|_t \frac{r}{v_{\text{ej}}(\tau)} + v_{\text{ej}}(\tau) \left(0 - \left. \frac{\partial \tau}{\partial r} \right|_t \right), \quad (31)$$

which yields

$$\left. \frac{\partial \tau}{\partial r} \right|_t = \frac{-1}{v_{\text{ej}} - r(v'_{\text{ej}}/v_{\text{ej}})}. \quad (32)$$

Then we find

$$\left. \frac{\partial}{\partial t} \right|_r = \left. \frac{\partial \tau}{\partial t} \right|_r \left. \frac{\partial}{\partial \tau} \right|_r + \left. \frac{\partial r}{\partial t} \right|_r \left. \frac{\partial}{\partial r} \right|_\tau = \frac{1}{1 - r(v'_{\text{ej}}/v_{\text{ej}}^2)} \left. \frac{\partial}{\partial \tau} \right|_r, \quad (33)$$

$$\left. \frac{\partial}{\partial r} \right|_t = \left. \frac{\partial \tau}{\partial r} \right|_t \left. \frac{\partial}{\partial \tau} \right|_r + \left. \frac{\partial r}{\partial r} \right|_t \left. \frac{\partial}{\partial r} \right|_\tau = \frac{-1}{v_{\text{ej}} - r(v'_{\text{ej}}/v_{\text{ej}})} \left. \frac{\partial}{\partial \tau} \right|_r + \left. \frac{\partial}{\partial r} \right|_\tau. \quad (34)$$

We substitute the equations (33) and (34) into the equation (27), and divide the whole equation by $\rho_{\text{ej}}\Gamma_{\text{ej}}v_{\text{ej}}$. Then we get

$$\frac{1}{v_{\text{ej}} - r(v'_{\text{ej}}/v_{\text{ej}})} \left. \frac{\partial}{\partial \tau} \right|_r \left[\ln \frac{1}{v_{\text{ej}}} \right] + \left. \frac{\partial}{\partial r} \right|_\tau [\ln \rho_{\text{ej}} + \ln(\Gamma_{\text{ej}}v_{\text{ej}})] + \frac{2}{r} = 0, \quad (35)$$

where the term $\ln(\Gamma_{\text{ej}}v_{\text{ej}})$ vanishes since it is a function of τ only. The equation (35) becomes

$$\frac{-v'_{\text{ej}}/v_{\text{ej}}}{v_{\text{ej}} - r(v'_{\text{ej}}/v_{\text{ej}})} + \left. \frac{\partial}{\partial r} \right|_\tau [\ln \rho_{\text{ej}}] + \frac{2}{r} = 0. \quad (36)$$

Finally, we integrate the equation (36) over r at fixed τ ,

$$\ln \left[1 - r \frac{v'_{\text{ej}}}{v_{\text{ej}}^2} \right] + \ln \rho_{\text{ej}} + 2 \ln r = \ln [f(\tau)], \quad (37)$$

where $f(\tau)$ is an arbitrary positive function of τ . Thus we find an analytical solution of the continuity equation for stratified ejecta,

$$\rho_{\text{ej}}(\tau, r) = \frac{f(\tau)}{r^2} \left[1 - r \frac{v'_{\text{ej}}}{v_{\text{ej}}^2} \right]^{-1} = \frac{f(\tau)}{r^2} \left[1 - \frac{r}{c} \frac{\Gamma'_{\text{ej}}}{(\Gamma_{\text{ej}}^2 - 1)^{3/2}} \right]^{-1}. \quad (38)$$

Here we have used the relation $v'_{\text{ej}}(\tau) = (c^2/v_{\text{ej}})(\Gamma'_{\text{ej}}/\Gamma_{\text{ej}}^3)$. The function $f(\tau)$ is determined below by the initial profile of ejecta near the center of the burst. The factor $1/r^2$ represents an overall side-expansion in 3 dimensional space. The remaining factor inside the brackets is responsible for a local spreadout of the ejecta due to its stratification. For 1 dimensional plane-parallel symmetry, the solution ρ_{ej} remains the same as above, except that there is no $1/r^2$ factor.

3.1.2. Initial profile of the ejecta

The τ -shell of energy $\delta E_{\text{ej}}(\tau)$, ejected at an ejection time τ , coasts with its Lorentz factor $\Gamma_{\text{ej}}(\tau)$. The initial profile of the ejected flow is set by the central engine of the explosion. Note that it is completely described by two functions; $\Gamma_{\text{ej}}(\tau)$ and $L_{\text{ej}}(\tau) \equiv dE_{\text{ej}}/d\tau$. Here the luminosity $L_{\text{ej}}(\tau)$ is related to the mass flow rate $\dot{M}(\tau)$ as $L_{\text{ej}} = \Gamma_{\text{ej}} \dot{M} c^2$. For small radii r , the mass flow rate is given by $\dot{M} = (4\pi r^2 v_{\text{ej}}) (\rho_{\text{ej}} \Gamma_{\text{ej}})$. Then the initial profile of ejecta density ρ_{ej} at the burst place is expressed as

$$\rho_{\text{ej}}(\tau, r) = \frac{L_{\text{ej}}}{4\pi r^2 v_{\text{ej}} \Gamma_{\text{ej}}^2 c^2}. \quad (39)$$

The solution (38) has a limiting form $\rho_{\text{ej}} = f(\tau)/r^2$ for small radii r . Thus we determine the function $f(\tau)$,

$$f(\tau) = \frac{L_{\text{ej}}}{4\pi v_{\text{ej}} \Gamma_{\text{ej}}^2 c^2} = \frac{\dot{M}}{4\pi v_{\text{ej}} \Gamma_{\text{ej}}}. \quad (40)$$

Hence the ejecta density is derived as

$$\rho_{\text{ej}}(\tau, r) = \frac{L_{\text{ej}}(\tau)}{4\pi r^2 v_{\text{ej}} \Gamma_{\text{ej}}^2 c^2} \left[1 - \frac{r}{c} \frac{\Gamma'_{\text{ej}}}{(\Gamma_{\text{ej}}^2 - 1)^{3/2}} \right]^{-1}. \quad (41)$$

The solution (41) is exact; we remark, however, that $\Gamma'_{\text{ej}}(\tau) \leq 0$ is assumed in the derivation. For given $\Gamma_{\text{ej}}(\tau)$ and $L_{\text{ej}}(\tau)$, the solution (41) allows us to fully understand the subsequent evolution of the ejected flow. The solution (41) is presented in Uhm & Beloborodov (2007) with no derivation.

3.2. Jump conditions of the FS and RS

In Section 2, we derived a simple form of jump conditions for shocks of arbitrary strength. We apply those jump conditions to the FS and RS of the blast wave, treating the gas in the blast as monoenergetic.

The Lorentz factors γ_1 and γ_2 are measured in the rest frame of the FS. As the ambient medium is at rest in the lab. frame, we notice that

$$\gamma_1 = \Gamma_f, \quad \gamma_2 = (1 - \beta\beta_f)\Gamma\Gamma_f, \quad \text{and} \quad \gamma_{12} = \Gamma. \quad (42)$$

The relative Lorentz factor $\gamma_{12} = \Gamma$ describes the shock strength of the FS. Then the jump conditions of the FS read

$$\gamma_1^2 = \frac{(4\Gamma^2 - 1)^2}{8\Gamma^2 + 1} \quad \text{or} \quad \beta_1 = \frac{4\beta}{\beta^2 + 3}, \quad (43)$$

$$\gamma_2^2 = \frac{9\Gamma^2}{8\Gamma^2 + 1} \quad \text{or} \quad \beta_2 = \frac{\beta}{3}, \quad (44)$$

$$p_2 = \frac{4}{3}(\Gamma^2 - 1)\rho_1 c^2, \quad \kappa_2 = \frac{1}{3}\left(1 + \frac{1}{\Gamma}\right), \quad (45)$$

$$\rho_2 = 4\Gamma\rho_1, \quad e_2 = 4\Gamma^2\rho_1 c^2. \quad (46)$$

Thus the Lorentz factor Γ_f and the thermodynamic quantities ρ_2 , e_2 , p_2 , and κ_2 immediately behind the FS are found in terms of Γ and ρ_1 . Here ρ_1 should be evaluated for the ambient medium immediately ahead the FS, which we denote by $\rho_1(\text{FS})$.

The RS is described by the same set of jump conditions when index 1 is replaced by 4 and index 2 by 3. The Lorentz factors γ_3 and γ_4 are measured in the rest frame of the RS,

$$\gamma_3 = (1 - \beta\beta_r)\Gamma\Gamma_r, \quad \text{and} \quad \gamma_4 = (1 - \beta_{\text{ej}}\beta_r)\Gamma_{\text{ej}}\Gamma_r. \quad (47)$$

The shock strength of the RS is described by the relative Lorentz factor γ_{43} ,

$$\gamma_{43} = (1 - \beta_4\beta_3)\gamma_4\gamma_3 = (1 - \beta\beta_{\text{ej}})\Gamma\Gamma_{\text{ej}}. \quad (48)$$

Then the jump conditions of the RS read

$$\gamma_4^2 = \frac{(4\gamma_{43}^2 - 1)^2}{8\gamma_{43}^2 + 1} \quad \text{or} \quad \beta_4 = \frac{4\beta_{43}}{\beta_{43}^2 + 3}, \quad (49)$$

$$\gamma_3^2 = \frac{9\gamma_{43}^2}{8\gamma_{43}^2 + 1} \quad \text{or} \quad \beta_3 = \frac{\beta_{43}}{3}, \quad (50)$$

$$p_3 = \frac{4}{3}(\gamma_{43}^2 - 1)\rho_4 c^2, \quad \kappa_3 = \frac{1}{3}\left(1 + \frac{1}{\gamma_{43}}\right), \quad (51)$$

$$\rho_3 = 4\gamma_{43}\rho_4, \quad e_3 = 4\gamma_{43}^2\rho_4 c^2. \quad (52)$$

The equation (47) yields the Lorentz factor Γ_r ,

$$\Gamma_r = (1 - \beta\beta_3) \Gamma\gamma_3 = (1 - \beta_{\text{ej}}\beta_4) \Gamma_{\text{ej}}\gamma_4, \quad (53)$$

where γ_3 and γ_4 are now given in terms of $\gamma_{43} = (1 - \beta\beta_{\text{ej}}) \Gamma\Gamma_{\text{ej}}$ above. Thus the Lorentz factor Γ_r and the thermodynamic quantities ρ_3 , e_3 , p_3 , and κ_3 immediately behind the RS are found in terms of Γ , Γ_{ej} , and ρ_4 . Here Γ_{ej} and ρ_4 should be evaluated for the shell immediately ahead the RS, which we denote by $\Gamma_{\text{ej}}(\text{RS})$ and $\rho_4(\text{RS}) \equiv \rho_{\text{ej}}(\text{RS})$ respectively.

Let the RS be located at radius r_r and sweep up the τ_r -shell in the ejecta when the FS is located at radius r_f ; the subscripts r and f refer to the RS and FS, respectively. When three functions $\rho_1(r)$, $\Gamma_{\text{ej}}(\tau)$, and $L_{\text{ej}}(\tau)$ are known, we find then $\rho_1(\text{FS}) = \rho_1(r_f)$, $\Gamma_{\text{ej}}(\text{RS}) = \Gamma_{\text{ej}}(\tau_r)$, and $\rho_{\text{ej}}(\text{RS}) = \rho_{\text{ej}}(\tau_r, r_r)$; the ejecta density $\rho_{\text{ej}}(\text{RS})$ is given by the solution (41) of the continuity equation for ejecta.

Thus the Lorentz factor Γ becomes the only free parameter for the blast wave with known input functions ρ_1 , Γ_{ej} , and L_{ej} . This is justified since we are given 6 independent equations (3 plus 3 jump conditions) for 7 unknowns, which are Γ , Γ_f , Γ_r , two independent thermodynamic quantities describing the gas behind the FS, and another two for the gas behind the RS.

3.3. Trajectory of the RS through ejecta

The path of the RS needs to be consistently tracked, as it propagates through the ejecta. Consider the RS located at radius $r_r(t)$ at time t , sweeping up the $\tau_r(t)$ -shell. The equation (28) gives the radius of the τ_r -shell at time t , which equals $r_r(t)$; $r_r(t) = v_{\text{ej}}(\tau_r[t])$ ($t - \tau_r[t]$). Then we find the velocity v_r of the RS,

$$v_r \equiv \frac{dr_r}{dt} = v'_{\text{ej}}(\tau_r) \frac{d\tau_r}{dt} \frac{r_r}{v_{\text{ej}}(\tau_r)} + v_{\text{ej}}(\tau_r) \left(1 - \frac{d\tau_r}{dt}\right) \quad (54)$$

$$= v_{\text{ej}}(\tau_r) - v_{\text{ej}}(\tau_r) \left[1 - r_r \frac{v'_{\text{ej}}(\tau_r)}{v_{\text{ej}}^2(\tau_r)}\right] \frac{d\tau_r}{dt}. \quad (55)$$

Using the relation

$$\frac{d\tau_r}{dt} = \frac{dr_r}{dt} \frac{d\tau_r}{dr_r} = v_r \frac{d\tau_r}{dr_r}, \quad (56)$$

we find a differential equation for $d\tau_r/dr_r$,

$$\frac{d\tau_r}{dr_r} = \left(\frac{1}{v_r} - \frac{1}{v_{\text{ej}}(\tau_r)}\right) \left[1 - r_r \frac{v'_{\text{ej}}(\tau_r)}{v_{\text{ej}}^2(\tau_r)}\right]^{-1}. \quad (57)$$

The equation (53) gives the velocity v_r in terms of Γ and $\Gamma_{\text{ej}}(\tau_r)$. Thus the equation (57) allows us to follow the trajectory of the RS through ejecta when Γ is known; for an infinitesimal displacement δr_r of the RS, we numerically solve the equation (57) to find $\delta \tau_r$.

The Lorentz factor Γ is determined below by two different methods; (1) customary pressure balance (see Section 3.5) and (2) the mechanical model (see Section 4). We demonstrate that the method (1) does not satisfy the energy-conservation law for adiabatic blast waves.

3.4. Adiabatic blast

As the blast wave propagates through the ambient medium, the blast grows and the gas in the blast evolves hydrodynamically. A simple way of dealing with an *adiabatic* evolution of the blast is described here. Since we treat the gas as monoenergetic, we first study the adiabatic process of a monoenergetic gas.

3.4.1. Adiabatic process of a monoenergetic gas

Consider a relativistic monoenergetic gas, which has the pressure p , energy density e , mean Lorentz factor $\bar{\gamma}$, volume V , number density n , and particle number N . An adiabatic process of the gas is defined by $d(eV) = -p dV$. When the particle number is conserved, we have $N = nV = \text{const}$, or $dV = -N dn/n^2$. Recalling the equation (19) for p and e of the monoenergetic gas, we find

$$d(nV \bar{\gamma} mc^2) = n mc^2 \frac{\bar{\gamma}^2 - 1}{3\bar{\gamma}} \left[\frac{N}{n^2} dn \right], \quad (58)$$

which yields

$$\frac{3\bar{\gamma}}{(\bar{\gamma}^2 - 1)} d\bar{\gamma} = \frac{1}{n} dn. \quad (59)$$

Here m denotes the particle mass in the gas. We integrate the equation (59) to find

$$n \propto (\bar{\gamma}^2 - 1)^{3/2} \quad \text{and} \quad p \propto \frac{1}{\bar{\gamma}} (\bar{\gamma}^2 - 1)^{5/2}. \quad (60)$$

Notice that $p \propto \bar{\gamma}^4$ is verified for the adiabatic process of an ultra-relativistic gas $\bar{\gamma} \gg 1$. Using the equation (20), i.e., $\kappa = \frac{1}{3}(1 + 1/\bar{\gamma})$, or $\bar{\gamma} = 1/(3\kappa - 1)$, we re-write the relation (60) as

$$p \propto \frac{\kappa^{5/2} (\frac{2}{3} - \kappa)^{5/2}}{(\kappa - \frac{1}{3})^4} \equiv p_m(\kappa). \quad (61)$$

Here we have defined the function $p_m(\kappa)$ for the right-hand side. The function $p_m(\kappa)$ is monotonically decreasing in its valid range, $\frac{1}{3} < \kappa < \frac{2}{3}$. The proportionality constant in the equation (61) is related to the entropy of the gas, which is conserved for the adiabatic process.

3.4.2. Evolution of adiabatic blast

We discretize the external ambient medium and ejecta into spherical mass shells δm , and use a Lagrangian description for the blast wave. Each δm is impulsively heated at some point by a shock front (FS or RS), acquiring its initial pressure p and quantity κ , which are given by the jump conditions (see Section 3.2). Using the equation (61), we can track the subsequent adiabatic evolution of each δm if we know the evolution of its pressure; the initial p and κ determine the proportionality constant, and we find numerically the new quantity κ when δm is at new pressure p . All other thermodynamic quantities of δm can then be found accordingly. For instance, the volume δV of the mass shell is obtained as

$$\delta V = \frac{mc^2}{p} \frac{(\bar{\gamma}^2 - 1)}{3\bar{\gamma}} \delta N = \frac{mc^2}{p} \frac{\kappa(\frac{2}{3} - \kappa)}{(\kappa - \frac{1}{3})} \delta N, \quad (62)$$

using the equation (19) and $\bar{\gamma} = 1/(3\kappa - 1)$. This volume δV is defined in the rest frame of the mass shell. The particle number δN of the mass shell is calculated when δm is shocked by a shock front, by making use of the particle number flux in the equation (2).

3.4.3. Energy of the blast

We may then calculate the energy of the blast. When the blast has an instantaneous Lorentz factor Γ , the total energy of the entire blast is evaluated in the lab. frame by integrating the 00-component of energy-momentum tensor over the volume of each δm :

$$E_{\text{blast}} = \sum_{\{\delta m\}} [\Gamma^2 (e + p) - p] \left(\frac{\delta V}{\Gamma} \right) = \sum_{\{\delta m\}} \left[\Gamma e \delta V + \left(\Gamma - \frac{1}{\Gamma} \right) p \delta V \right]. \quad (63)$$

Due to the Lorentz contraction, $\delta V/\Gamma$ is the volume of δm in the lab. frame. Replacing the energy $e \delta V$ by $(\bar{\gamma} mc^2) \delta N$ and using the equation (62) for $p \delta V$, we find

$$E_{\text{blast}} = \sum_{\{\delta m\}} \left[\Gamma \bar{\gamma} + \frac{1}{3} \left(\Gamma - \frac{1}{\Gamma} \right) \left(\bar{\gamma} - \frac{1}{\bar{\gamma}} \right) \right] (mc^2 \delta N). \quad (64)$$

We emphasize that the second term here needs to be included in order to correctly express the energy of blast. For relativistic blast waves, $\Gamma^2 \gg 1$, the equation (64) becomes

$$E_{\text{blast}} \simeq \sum_{\{\delta m\}} \Gamma \left[\frac{1}{3} \left(4\bar{\gamma} - \frac{1}{\bar{\gamma}} \right) \right] (mc^2 \delta N) = \sum_{\{\delta m\}} \Gamma \left[\frac{(1 - \kappa)(3\kappa + 1)}{(3\kappa - 1)} \right] (mc^2 \delta N). \quad (65)$$

The energy E_4 of unshocked ejecta (region 4) is easily found as $E_4 = \int_{\tau_r}^{\infty} L_{\text{ej}}(\tau) d\tau$, where τ_r indicates the location of the RS in the ejecta. The energy of region 1 is negligible since the ambient medium is at rest in the lab. frame. Thus the total energy of the entire system is obtained as $E_{\text{tot}} = E_{\text{blast}} + E_4$.

3.5. Customary pressure balance: $p_f = p_r$

A customary approximation assumes a pressure balance across the blast wave; i.e., the pressure p_f at the FS is equated to the pressure p_r at the RS. The equations (45) and (51) give the pressures $p_f = p_2$ and $p_r = p_3$,

$$p_f = \frac{4}{3} (\Gamma^2 - 1) \rho_1 c^2, \quad p_r = \frac{4}{3} (\gamma_{43}^2 - 1) \rho_4 c^2. \quad (66)$$

For relativistic blast waves ($\Gamma_{\text{ej}} \gg 1$ and $\Gamma \gg 1$), the pressure balance $p_f = p_r$ determines the instantaneous Γ of the blast wave (Beloborodov & Uhm 2006),

$$\Gamma = \Gamma_{\text{ej}} \left[1 + 2 \Gamma_{\text{ej}} \left(\frac{\rho_1}{\rho_{\text{ej}}} \right)^{1/2} \right]^{-1/2}, \quad p_f = p_r, \quad (67)$$

denoting $\rho_4 = \rho_{\text{ej}}$. Recall that $\rho_1 = \rho_1(\text{FS})$, $\rho_{\text{ej}} = \rho_{\text{ej}}(\text{RS})$, and $\Gamma_{\text{ej}} = \Gamma_{\text{ej}}(\text{RS})$ should be used here; see Section 3.2.

The solution (67) indicates that the dynamical evolution of the blast wave is determined by purely input parameters ρ_1 , ρ_{ej} , and Γ_{ej} of regions 1 and 4. The solution Γ has no information on the thermodynamical status of the gas in blast. This observation makes us to doubt the validity of the solution (67). The approximation $p_f = p_r$ itself is then doubted. As we demonstrate below, the solution (67) in fact does *not* satisfy the energy conservation for adiabatic blast waves.

3.5.1. Example model

The initial setup of an explosion is specified by three functions ρ_1 , Γ_{ej} , and L_{ej} , which can be arbitrary as long as $\Gamma'_{\text{ej}}(\tau) \leq 0$. We consider a simple example model that assumes

$$L_{\text{ej}}(\tau) = L_0 = 10^{52} \text{ erg/s}, \quad \Gamma_{\text{ej}}(\tau) = 500 - 9\tau, \quad 0 \leq \tau \leq \tau_b = 50 \text{ s}. \quad (68)$$

The luminosity L_{ej} remains at a constant L_0 during the duration τ_b of the burst. The Lorentz factor Γ_{ej} decreases linearly from 500 to 50. The total energy E_b of the burst is simply $E_b = L_0 \tau_b$. The ambient medium is assumed to have a uniform density $n_1 = \rho_1/m_p = 1 \text{ cm}^{-3}$. Here m_p is the proton mass.

For this example burst, we find the evolution of the blast wave as follows. Suppose that, at time t , the RS is located at radius $r_r(t)$, the FS is located at radius $r_f(t)$, the $\tau_r(t)$ -shell passes through the RS, and the blast has the Lorentz factor $\Gamma(t)$. We evaluate $\rho_1(\text{FS}) = \rho_1(r_f)$, $\Gamma_{\text{ej}}(\text{RS}) = \Gamma_{\text{ej}}(\tau_r)$, and $\rho_{\text{ej}}(\text{RS}) = \rho_{\text{ej}}(\tau_r, r_r)$ (the equation [41]), which in turn gives γ_{43} , γ_3 , Γ_r (the equation [53]), and Γ_f . For an infinitesimal displacement δr_r of the RS, we numerically solve the equation (57) to find $\delta \tau_r$. The equation (28), $r = v_{\text{ej}}(\tau)(t - \tau)$, gives then the time for the new location of the RS ($r_r + \delta r_r$ in radius and $\tau_r + \delta \tau_r$ in ejecta). Thus we find the time interval δt for this displacement δr_r . The new location of the FS is found by its displacement during δt with the velocity given by its Lorentz factor Γ_f . We evaluate $\rho_1(\text{FS})$, $\Gamma_{\text{ej}}(\text{RS})$, and $\rho_{\text{ej}}(\text{RS})$ again for the new location. Then the solution (67) determines the Lorentz factor Γ of the blast for the new location. The result is shown in Figure 3.

The solution (67) also determines the pressure $p = p_f = p_r$ across the blast. This enables us to track the adiabatic evolution of the mass shells in blast (see Section 3.4.2), and to find the total energy E_{tot} of the entire system (see Section 3.4.3). In Figure 4, we show the resulting total energy E_{tot} . Apparently, the energy conservation is not satisfied; E_{tot} has decreased by a factor of 5 by the moment the RS crosses the last shell ($\tau = 50 \text{ s}$) in the ejecta.

3.5.2. What is wrong?

The spherical expansion of ejecta was completely described by the solution (41). The propagation of the RS through ejecta was found self-consistently by the equation (57). The conservation laws of energy-momentum tensor and mass flux were explicitly applied across both the FS and the RS (the jump conditions). The gas in blast, however, was not required to obey those conservation laws; i.e., the pressure balance $p_f = p_r$ omits the physics laws

that should govern the gas in blast. Evidently, this is why the energy conservation for the adiabatic blast wave was not satisfied above. Notice that one among three independent conservation laws was effectively applied to the blast, since we tracked the adiabatic evolution of the mass shells in blast in order to find the total energy of the system.

Adiabatic expansion of the gas in blast implies a pdV work done to the gas itself. This work needs to be converted to the kinetic energy of the bulk motion of blast. Clearly, such a conversion mechanism is absent from the solution (67) as it depends only on input parameters of regions 1 and 4. A correct modeling for the blast wave should indicate a mechanism that the dynamical variable Γ is affected by the thermodynamic status of the gas in blast.

Applying the conservation laws of energy-momentum tensor and mass flux to everywhere on the blast, we developed a simple “mechanical model” for the blast wave (Beloborodov & Uhm 2006). The mechanical model successfully resolves the energy-violation problem, because it replaces the pressure balance $p_f = p_r$ by the physics laws. We summarize the model below including more detailed equations.

4. Mechanical model for relativistic blast waves

The gas in the blast wave flows radially with the 4-velocity $u^\alpha = \gamma(1, \beta, 0, 0)$ in spherical coordinates (ct, r, θ, ϕ) , where the metric $ds^2 = -c^2 dt^2 + dr^2 + r^2 d\theta^2 + r^2 \sin^2 \theta d\phi^2$ has the determinant $g = -r^4 \sin^2 \theta$. For any scalar function f , the covariant divergence of $f u^\alpha$ is given as (e.g., see Carroll 2004),

$$\nabla_\alpha(f u^\alpha) = \frac{1}{\sqrt{-g}} \partial_\alpha (\sqrt{-g} f u^\alpha) = \frac{1}{r^2} \partial_\alpha (r^2 f u^\alpha) \quad (69)$$

$$= \frac{1}{r^2 c} \frac{d}{dt} (r^2 f \gamma) + f \gamma \frac{\partial \beta}{\partial r}, \quad (70)$$

where $\frac{d}{dt} \equiv \frac{\partial}{\partial t} + c\beta \frac{\partial}{\partial r}$ is the convective derivative. The rest-mass conservation $\nabla_\alpha(\rho u^\alpha) = 0$ reads then

$$\frac{1}{r^2 c} \frac{d}{dt} (r^2 \rho \gamma) + \rho \gamma \frac{\partial \beta}{\partial r} = 0. \quad (71)$$

The energy-momentum tensor for a perfect fluid is written as

$$T^{\alpha\mu} = h u^\alpha u^\mu + g^{\alpha\mu} p, \quad h \equiv e + p. \quad (72)$$

The conservation $\nabla_\mu T_\alpha^\mu = \nabla_\mu (h u_\alpha u^\mu + \delta_\alpha^\mu p) = 0$ gives two independent equations ($\alpha = 0, 1$)

$$\frac{1}{r^2 c} \frac{d}{dt} (r^2 h \gamma u_\alpha) + h \gamma u_\alpha \frac{\partial \beta}{\partial r} + \partial_\alpha p = 0, \quad (73)$$

where the equation (70) is used. For $\alpha = 1$, the equation (73) becomes

$$\frac{1}{r^2 c} \frac{d}{dt} (r^2 h \gamma^2 \beta) = -\frac{\partial p}{\partial r} - h \gamma^2 \beta \frac{\partial \beta}{\partial r}. \quad (74)$$

Instead of $\nabla_\mu T_0^\mu = 0$ ($\alpha = 0$), we use the projection $u^\alpha \nabla_\mu T_\alpha^\mu = 0$. Since $u^\alpha u_\alpha = -1$ and $u^\alpha \nabla_\mu u_\alpha = 0$, the projection becomes

$$\nabla_\mu (h u^\mu) = u^\alpha \nabla_\alpha p, \quad (75)$$

which yields

$$\frac{1}{r^2 c} \frac{d}{dt} (r^2 h \gamma) = \frac{\gamma}{c} \frac{dp}{dt} - h \gamma \frac{\partial \beta}{\partial r}. \quad (76)$$

We apply three independent equations (71), (74), and (76) to the gas between the FS and the RS, and make the approximation

$$\gamma(t, r) = \Gamma(t), \quad \partial \beta / \partial r = 0, \quad r_r < r < r_f, \quad (77)$$

where $r_r(t)$ and $r_f(t)$ are the instantaneous radii of the RS and FS, respectively. Then the integration of three equations (71), (74), and (76) over r between r_r and r_f (at $t = \text{const}$) yields

$$\frac{1}{r^2 c} \frac{d}{dt} (r^2 \Sigma \Gamma) - \Gamma [\rho_r (\beta - \beta_r) + \rho_f (\beta_f - \beta)] = 0, \quad (78)$$

$$\frac{1}{r^2 c} \frac{d}{dt} (r^2 H \Gamma^2 \beta) - \Gamma^2 \beta [h_r (\beta - \beta_r) + h_f (\beta_f - \beta)] = p_r - p_f, \quad (79)$$

$$\frac{1}{r^2 c} \frac{d}{dt} (r^2 H \Gamma) - \Gamma [h_r (\beta - \beta_r) + h_f (\beta_f - \beta)] = \frac{\Gamma}{c} \frac{d}{dt} P - \Gamma [p_r (\beta - \beta_r) + p_f (\beta_f - \beta)], \quad (80)$$

where $\Sigma \equiv \int_{r_r}^{r_f} \rho dr$, $H \equiv \int_{r_r}^{r_f} h dr$, $P \equiv \int_{r_r}^{r_f} p dr$, $c\beta_r = dr_r/dt$, and $c\beta_f = dr_f/dt$. Here we have used an identity for any function $f(t, r)$,

$$\int_{r_r(t)}^{r_f(t)} \left[\frac{d}{dt} f(t, r) \right] dr = \frac{d}{dt} \left[\int_{r_r(t)}^{r_f(t)} f(t, r) dr \right] - c [f_r(t) \{\beta(t) - \beta_r(t)\} + f_f(t) \{\beta_f(t) - \beta(t)\}], \quad (81)$$

where $f_r(t) \equiv f(t, r_r(t))$ and $f_f(t) \equiv f(t, r_f(t))$. The relativistic blast is a very thin shell, $r_f - r_r \sim r/\Gamma^2 \ll r$, so we used $r_f \approx r_r \approx r$ when calculating the integrals.

We simplify the equations (78)-(80) by making use of $\Gamma \gg 1$. The jump conditions at the FS give $\Gamma_f^2 = 2\Gamma^2$, $\beta_f - \beta = 1/(4\Gamma^2)$, $e_f = 3p_f$, and $h_f = e_f + p_f = 4p_f \gg \rho_f c^2$. The

convective derivative $d/dt = c\beta d/dr$ may be replaced by $c d/dr$ everywhere, and $\Gamma^2\beta$ by Γ^2 in the equation (79). Then we get

$$\frac{\Gamma}{r^2} \frac{d}{dr} (r^2 \Sigma \Gamma) = \rho_r (\beta - \beta_r) \Gamma^2 + \frac{1}{4} \rho_f, \quad (82)$$

$$\frac{1}{r^2} \frac{d}{dr} (r^2 H \Gamma^2) = h_r (\beta - \beta_r) \Gamma^2 + p_r, \quad (83)$$

$$\frac{\Gamma}{r^2} \frac{d}{dr} (r^2 H \Gamma) = \Gamma^2 \frac{dP}{dr} + (h_r - p_r) (\beta - \beta_r) \Gamma^2 + \frac{3}{4} p_f. \quad (84)$$

The FS jump conditions give

$$\rho_f = 4\Gamma \rho_1, \quad p_f = \frac{4}{3} \Gamma^2 \rho_1 c^2. \quad (85)$$

Recalling $\beta_3 = (\beta - \beta_r)/(1 - \beta\beta_r)$ and the RS jump condition $\beta_3 = \beta_{43}/3$, we find

$$\beta - \beta_r = \frac{\beta_{43}}{\Gamma^2 (3 - \beta\beta_{43})} = \frac{\beta_{43}}{\Gamma^2 (3 - \beta_{43})}, \quad (86)$$

where the second equality is valid for $\gamma_{43} \ll \Gamma$. For the relativistic blast wave, the Lorentz factor $\gamma_{43} = (1 - \beta\beta_{ej}) \Gamma \Gamma_{ej}$ becomes

$$\gamma_{43} = \frac{1}{2} \left(\frac{\Gamma_{ej}}{\Gamma} + \frac{\Gamma}{\Gamma_{ej}} \right), \quad \beta_{43} = \frac{\Gamma_{ej}^2 - \Gamma^2}{\Gamma_{ej}^2 + \Gamma^2}. \quad (87)$$

Then we find

$$\beta - \beta_r = \frac{\Gamma_{ej}^2 - \Gamma^2}{2\Gamma^2 (\Gamma_{ej}^2 + 2\Gamma^2)}. \quad (88)$$

The jump conditions at the RS are

$$\rho_r = 4\gamma_{43} \rho_{ej}, \quad e_r = 4\gamma_{43}^2 \rho_{ej} c^2, \quad p_r = \frac{4}{3} (\gamma_{43}^2 - 1) \rho_{ej} c^2, \quad (89)$$

which yield

$$\rho_r = 2 \left(\frac{\Gamma_{ej}}{\Gamma} + \frac{\Gamma}{\Gamma_{ej}} \right) \rho_{ej}, \quad p_r = \frac{1}{3} \left(\frac{\Gamma_{ej}}{\Gamma} - \frac{\Gamma}{\Gamma_{ej}} \right)^2 \rho_{ej} c^2, \quad (90)$$

$$h_r = \frac{4}{3} \left(\frac{\Gamma_{ej}^2}{\Gamma^2} + \frac{\Gamma^2}{\Gamma_{ej}^2} + 1 \right) \rho_{ej} c^2. \quad (91)$$

Here the equation (87) has been used.

This leaves four unknowns in the equations (82)-(84): Σ , H , P , and Γ . One more equation is required to close the set of coupled differential equations. We propose the following approximate relation,

$$H - \Sigma c^2 = 4P. \quad (92)$$

As shown in Beloborodov & Uhm (2006), it is accurate in the limits of both an ultra-relativistic RS and a non-relativistic RS, and should be a reasonable approximation in an intermediate case.

5. Discussion

A dynamical evolution of the blast wave is found for the mechanical model as follows. For an infinitesimal displacement of the blast, we numerically solve the coupled equations (82)-(84) and (92) of the mechanical model, and find the instantaneous Lorentz factor Γ and integrated quantities H , Σ , and P . We also solve the differential equation (57) to get the RS trajectory through the ejecta.

For the same example model as used for the customary pressure balance $p_r = p_f$, we find the blast-wave evolution. Recall that the example burst is described in the equation (68) and the ambient medium is assumed to have the density $n_1 = \rho_1/m_p = 1 \text{ cm}^{-3}$. The result found for the mechanical model is shown in Figure 5 (in solid lines); for comparison, the solution found for the pressure balance is shown together (in dotted lines). Notice that two sets of solutions differ significantly; in particular, the blast wave obtained for the mechanical model decelerates slower and propagates farther (see Panel c) until the RS arrives at the same last shell ($\tau = 50 \text{ s}$) in the ejecta (see Panel a). For the pressure balance, on the other hand, the energy loss shown in Figure 4 is responsible for the earlier deceleration of the blast wave.

The energy of the blast is easily found for the mechanical model; it is evaluated in the lab. frame by integrating the 00-component of energy-momentum tensor over volume,

$$E_{\text{blast}} = \int_{r_r}^{r_f} [\Gamma^2 (e + p) - p] (4\pi r^2 dr) \simeq 4\pi r^2 (\Gamma^2 H - P). \quad (93)$$

We find this blast energy for the same example model above, and show the result in Figure 6. The total energy E_{tot} of the entire system is precisely conserved; the mechanical model is indeed a successful remedy for the energy-violation problem.

The energy of the blast can alternatively be found by using the expression (64). In order to track the adiabatic evolution of the mass shells in blast (see Section 3.4.2) and to find the blast energy, we need to know a pressure profile for the mass shells. In case of the mechanical model, an instantaneous pressure profile for the blast may be approximated by a quadratic function of r ($r_r < r < r_f$), which (1) matches two boundary values (p_r at r_r and p_f at r_f) and (2) satisfies the integrated pressure P . The boundary values are met by

a quadratic function $p(r) = a(r - b)^2 + c$ with

$$b = \frac{1}{2}(r_f + r_r) - \frac{1}{2a} \frac{p_f - p_r}{r_f - r_r}, \quad (94)$$

$$c = \frac{1}{2}(p_f + p_r) - \frac{a}{4}(r_f - r_r)^2 - \frac{1}{4a} \left(\frac{p_f - p_r}{r_f - r_r} \right)^2. \quad (95)$$

The remaining unknown a is determined such that $P = \int_{r_r}^{r_f} p(r) dr$. An upper bound for a is required since $p(r)$ is positive everywhere on the blast; $a < (\sqrt{p_f} + \sqrt{p_r})^2 / (r_f - r_r)^2$.

We find this quadratic profile for the dynamical evolution shown in Figure 5 (i.e., the solid lines found for the mechanical model), and evaluate the expression (64) to find the blast energy. The result is shown in Figure 7. The total energy E_{tot} is conserved within about 5 % for this example. Thus the quadratic pressure profile should be a reasonably good approximation for the mechanical model.

We also calculate the synchrotron emission from both the FS-shocked and RS-shocked regions. We make use of the standard prescription of microphysical parameters (e.g., Piran 2004); ϵ_e (fraction of the shock energy that goes to electron acceleration), ϵ_B (magnetic parameter), and p (slope of the electron spectrum). We track the synchrotron emissivity of all shells on the blast; i.e., a radiative and adiabatic cooling of the electron spectrum is tracked for each shell, and an adiabatic evolution of shocked gas is tracked to give an evolution of magnetic field for each shell. The velocity and spherical curvature of the shells are also taken into account. A more detailed description will be presented elsewhere. The resulting afterglow light-curves are shown in Figure 8 (R-band) and Figure 9 (1 keV). We find that the two different blast-wave evolutions shown in Figure 5 yield significantly different sets of light-curves for the same example burst. In particular, the light-curves obtained with the pressure balance decrease earlier than those with the mechanical model, due to an energy loss seen in Figure 4.

A spherically symmetric formulation presented here becomes less accurate when the sideways expansion becomes important at late stages of the blast-wave evolution; i.e., $\Gamma \lesssim \theta_{\text{jet}}^{-1}$. In their relativistic hydrodynamical simulations, Meliani et al. (2007) showed that a 2D jet-like model decelerates earlier than its 1D isotropic counterpart when thermally induced expansions lead to significantly high lateral speeds. On the other hand, Zhang & MacFadyen (2009) showed that the sideways expansion is a very slow process and previous analytic works (Rhoads 1999; Sari et al. 1999) greatly overestimated the rate of the sideways expansion.

6. Conclusion

As the blast wave propagates, the strength of the RS wave exhibits a transition from non-relativistic to mildly-relativistic or relativistic regime (or vice versa). Thus, an EOS with a constant adiabatic index is not adequate for the RS-shocked region. We address that a more realistic EOS with a variable adiabatic index needs to be used for the gas in the RS-shocked region.

Following Mathews (1971), we consider a relativistic monoenergetic gas and find its EOS. We show that there is only 4.8 % of maximal difference in the quantity κ (pressure divided by internal energy density) when compared to a relativistic ideal gas. Then we show that jump conditions of relativistic hydrodynamical shocks simplify significantly for the monoenergetic gas (see Section 2). The simple form of jump conditions presented here is exact for a monoenergetic gas, and applies to shocks of arbitrary strength (relativistic, mildly-relativistic, or non-relativistic). We emphasize that its usage is not to be restricted to GRB blast waves; it can be applied to other areas of relativistic hydrodynamical shocks.

Then we present a semi-analytic formulation for relativistic blast waves with a long-lived RS. We describe in detail a complete set of tools for finding a dynamical evolution of the blast wave for a very general class of explosions. The ambient medium can have an arbitrary radial profile, and the explosion ejecta can also be arbitrary as long as $\Gamma'_{\text{ej}}(\tau) \leq 0$. We provide two different methods of finding dynamics of the blast wave: (1) customary pressure balance and (2) the mechanical model (Beloborodov & Uhm 2006). Using a simple example model, we show that the pressure balance across the blast wave does not satisfy the energy conservation for an adiabatic blast wave; the total energy is decreased by a factor of 5 in the case of the example model.

The mechanical model does not assume a pressure balance or proportionality across the blast wave (neither $p_f = p_r$ nor $p_f/p_r = \text{const.}$ is assumed). Instead, it finds the dynamics of the blast wave from a set of coupled differential equations that express the conservations of energy-momentum tensor and mass flux applied on the blast between the FS and RS. Using the same example model, we show that the energy conservation is satisfied for the mechanical model as expected.

We also show that the two methods yield very different dynamical evolutions of the blast wave and, as a result, very different afterglow light-curves. We conclude that the customary prescription of pressure balance poorly describes the dynamics of the blast wave with a long-lived RS and resulting afterglow light-curves are inaccurate in a significant manner.

The author is grateful to Andrei M. Beloborodov for numerous helpful discussions and

generous contributions to this work. The author is also grateful to Robert Mochkovitch, Frédéric Daigne, and the anonymous referee for helpful comments to improve the manuscript. This research was supported by the World Class University program (R32-2009-000-10130-0) of NRF/MEST of Korea.

REFERENCES

- Beloborodov, A. M., & Uhm, Z. L. 2006, *ApJ*, 651, L1
- Blandford, R. D., & McKee, C. F. 1976, *Phys. of Fluids*, 19, 1130
- Blumenthal, G. R., & Mathews, W. G. 1976, *ApJ*, 203, 714
- Carroll, S. M. 2004, *Spacetime and Geometry* (Addison Wesley)
- Greiner, W., Neise, L., & Stocker, H. 1995, *Thermodynamics and Statistical Mechanics* (Springer-Verlag)
- Kobayashi, S. 2000, *ApJ*, 545, 807
- Kobayashi, S., & Sari, R. 2000, *ApJ*, 542, 819
- Landau, L. D., & Lifshitz, E. M. 1959, *Fluid Mechanics* (Oxford: Pergamon)
- Mathews, W. G. 1971, *ApJ*, 165, 147
- Meliani, Z., Keppens, R., Casse, F., & Giannios, D. 2007, *MNRAS*, 376, 1189
- Meliani, Z., Sauty, C., Tsinganos, K., & Vlahakis, N. 2004, *A&A*, 425, 773
- Mészáros, P. 2006, *Rep. Prog. Phys.*, 69, 2259
- Mészáros, P., & Rees, M. J. 1997, *ApJ*, 476, 232
- Mészáros, P., & Rees, M. J. 1999, *MNRAS*, 306, L39
- Mignone, A., & McKinney, J. C. 2007, *MNRAS*, 378, 1118
- Mignone, A., Plewa, T., & Bodo, G. 2005, *ApJS*, 160, 199
- Piran, T. 2004, *Rev. Mod. Phys.*, 76, 1143
- Rees, M. J., & Mészáros, P. 1998, *ApJ*, 496, L1

- Rhoads, J. E. 1999, ApJ, 525, 737
- Sari, R., & Piran, T. 1995, ApJ, 455, L143
- Sari, R., & Piran, T. 1999a, ApJ, 517, L109
- Sari, R., & Piran, T. 1999b, ApJ, 520, 641
- Sari, R., Piran, T., & Halpern, J. P. 1999, ApJ, 519, L17
- Synge, J. L. 1957, The Relativistic Gas (Amsterdam: North-Holland)
- Taub, A. H. 1948, Phys. Rev., 74, 328
- Uhm, Z. L., & Beloborodov, A. M. 2007, ApJ, 665, L93.
- Zhang, W., & MacFadyen, A. 2009, ApJ, 698, 1261

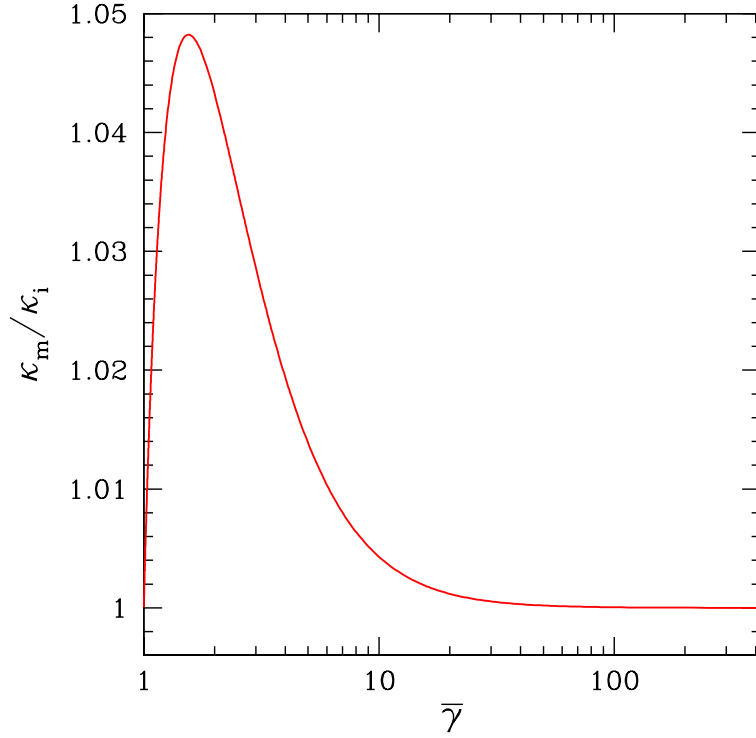


Fig. 1.— The ratio κ_m/κ_i as a function of the mean Lorentz factor $\bar{\gamma}$ of particles of a gas. The quantity κ is defined in the equation of state (5) for a relativistic gas. The subscripts i and m refer to a relativistic ideal gas and a monoenergetic gas, respectively. An expression for each κ_i and κ_m is derived in Section 2.2. Note that there is only 4.8 % of maximal difference between the two at about $\bar{\gamma} = 1.6$.

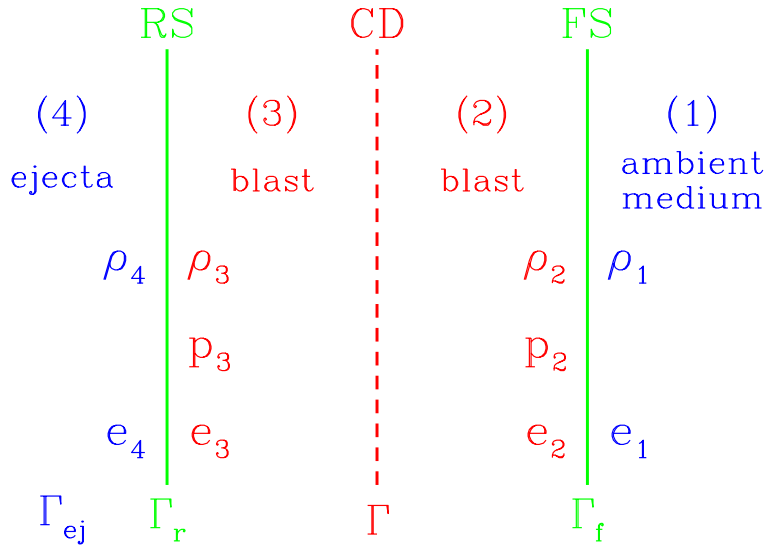


Fig. 2.— An illustrative diagram of 4 regions in a blast wave. The forward shock (FS) sweeps up the external ambient medium (region 1) and the reverse shock (RS) propagates through the ejecta (region 4). The shocked ambient medium (region 2) is separated from the shocked ejecta (region 3) by a contact discontinuity (CD). Two shocked regions 2 and 3 between the FS and RS are ‘hot’ and called the blast. The pre-shock regions 1 and 4 are ‘cold’, having no pressure. The entire blast is assumed to have a common Lorentz factor Γ .

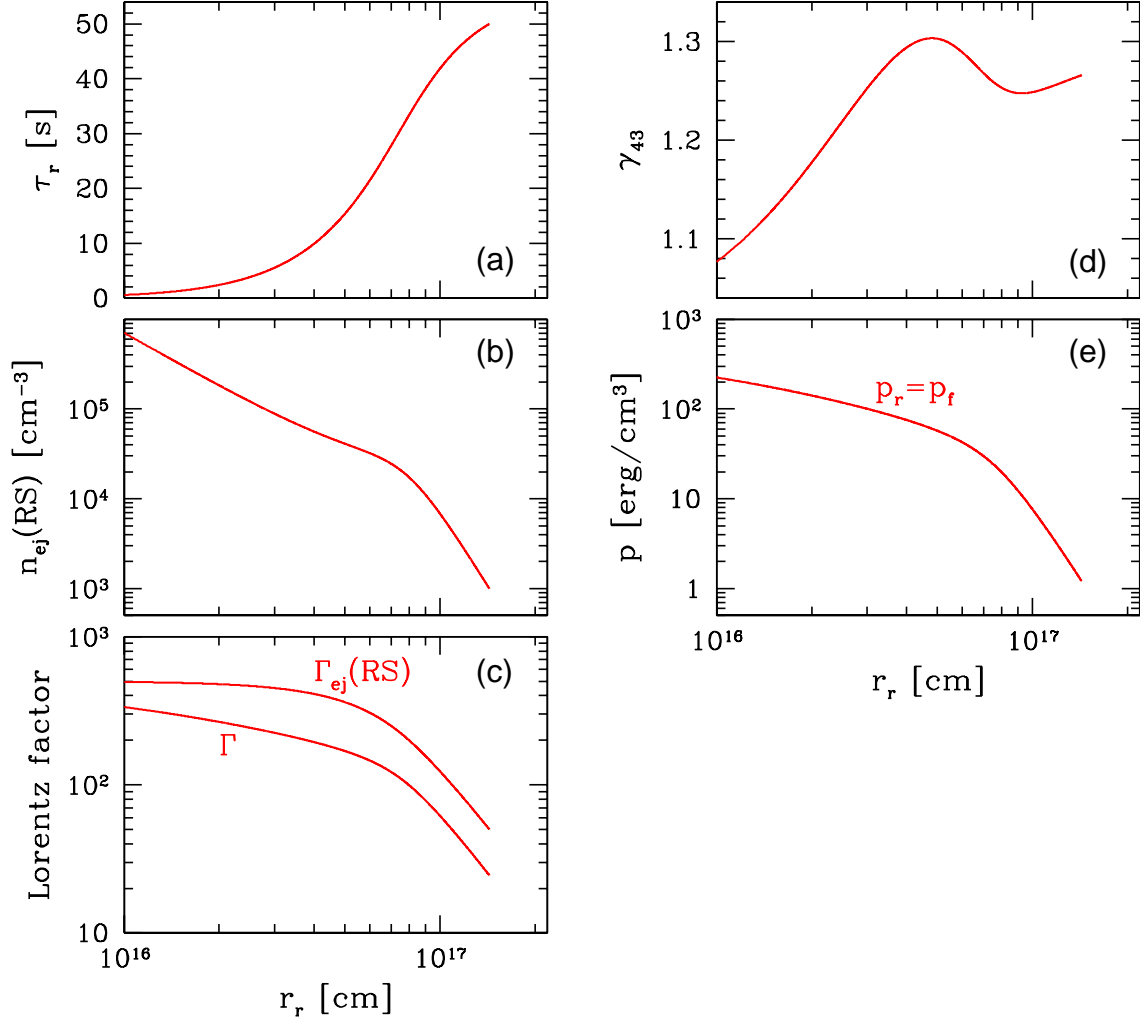


Fig. 3.— A numerical solution for the blast-wave driven by the example burst specified in the equation (68); $L_{\text{ej}}(\tau) = L_0 = 10^{52}$ erg/s and $\Gamma_{\text{ej}}(\tau) = 500 - 9\tau$ for $0 \leq \tau \leq \tau_b = 50$ s. The ambient medium density is assumed to be $n_1 = \rho_1/m_p = 1 \text{ cm}^{-3}$. Here m_p is the proton mass. This solution is found as described in Section 3.5.1, using the equation (67) of the pressure balance $p_r = p_f$. Panel (a) shows the τ_r -shell passing through the RS at radius r_r . Panel (b) is the ejecta density $n_{\text{ej}}(\text{RS}) = \rho_{\text{ej}}(\text{RS})/m_p$ of the τ_r -shell. Panel (c) shows the Lorentz factor $\Gamma_{\text{ej}}(\text{RS})$ of the τ_r -shell and Γ of the blast, which yields the relative Lorentz factor γ_{43} in panel (d). Panel (e) shows that a pressure balance $p = p_r = p_f$ is assumed across the blast. However, this numerical solution does not satisfy the energy-conservation law for the adiabatic blast wave; see Figure 4.

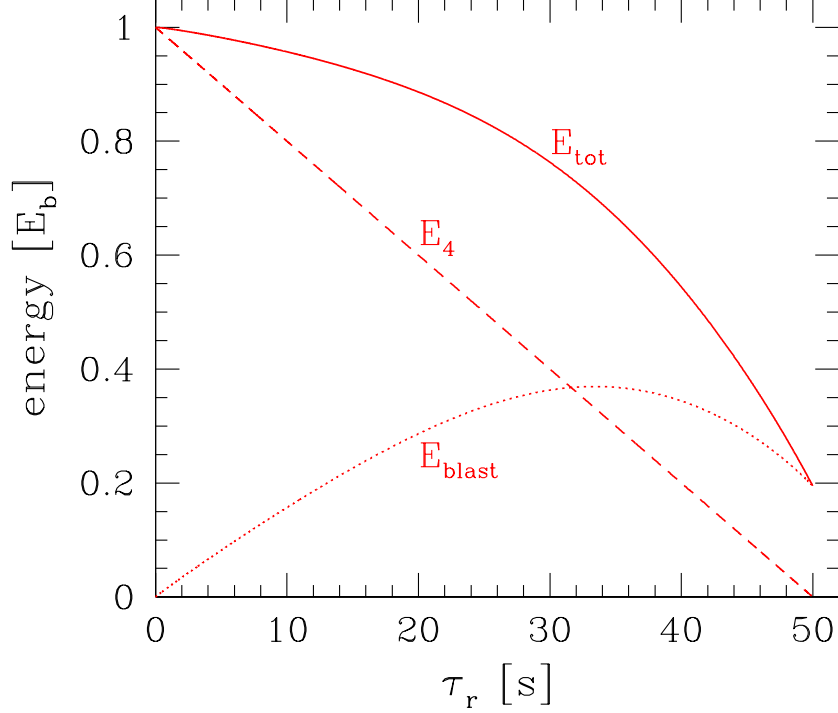


Fig. 4.— The energy E_{blast} of the blast (dotted line), the energy E_4 of region 4 (dashed line), and the total energy E_{tot} of the entire system (solid line; $E_{\text{tot}} = E_{\text{blast}} + E_4$) for the blast-wave evolution shown in Figure 3. The dynamical evolution in Figure 3 is found by using the pressure balance $p_r = p_f$ for the example burst specified in the equation (68); $L_{\text{ej}}(\tau) = L_0 = 10^{52}$ erg/s and $\Gamma_{\text{ej}}(\tau) = 500 - 9\tau$ for $0 \leq \tau \leq \tau_b = 50$ s. The ambient medium density is assumed to be $n_1 = \rho_1/m_p = 1 \text{ cm}^{-3}$. The energy E_b here is the total energy ejected by the burst; $E_b = L_0\tau_b = 5 \times 10^{53}$ ergs. The energies E_{blast} , E_4 , and E_{tot} are shown in the units of E_b for the τ_r -shell, i.e., the location of the RS in the ejecta. We precisely track the adiabatic evolution of the mass shells in the blast (see Section 3.4.2), and find the total energy E_{tot} of the entire system (see Section 3.4.3). However, the resulting total energy is clearly not conserved above; it has decreased by a factor of 5 by the moment the RS crosses the last shell ($\tau = 50$ s) in the ejecta. This demonstrates that the solution (67) derived from the pressure balance $p_f = p_r$ violates the energy-conservation law significantly for the adiabatic blast wave.

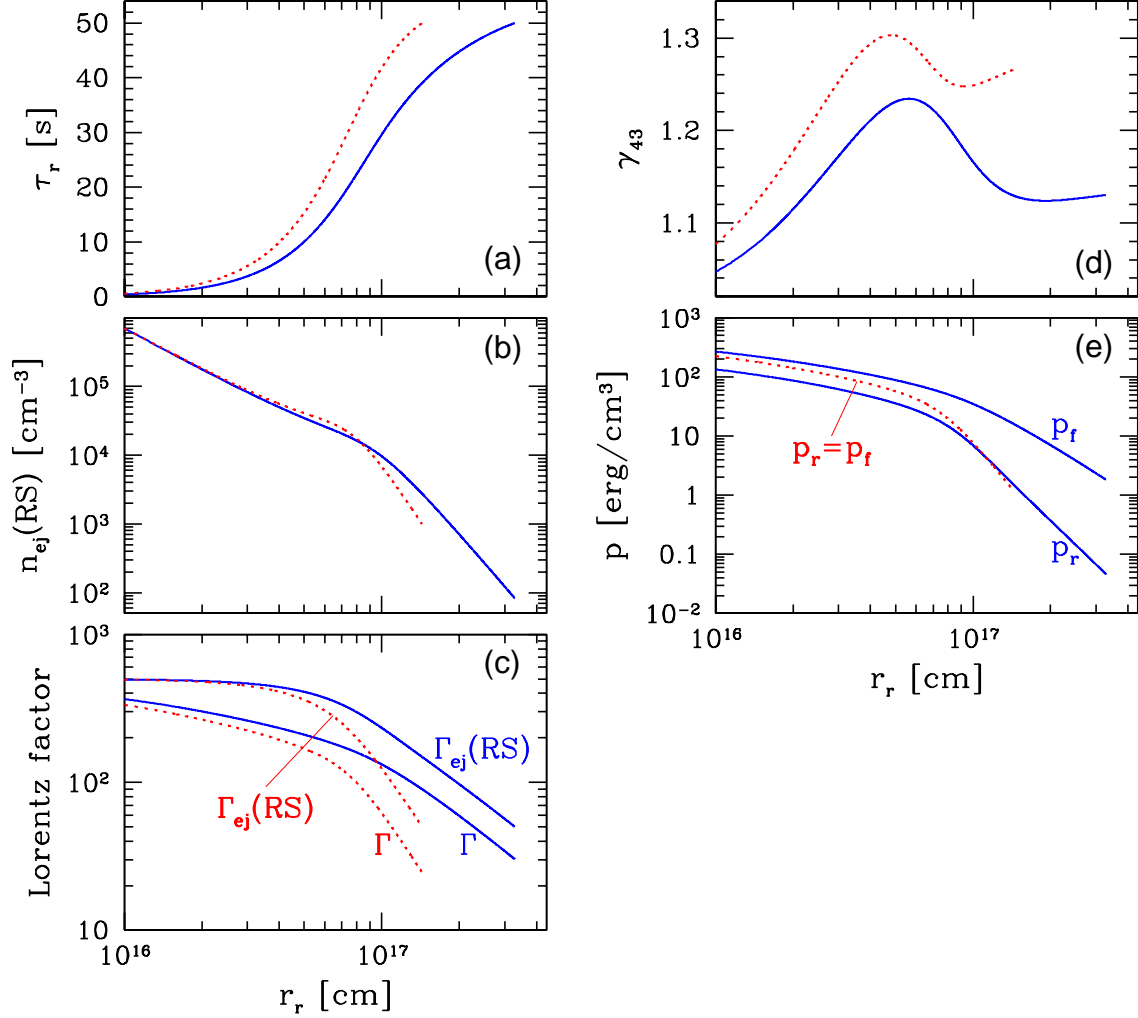


Fig. 5.— Numerical solutions for the blast-wave driven by the same example burst described in the equation (68). The ambient medium density is also the same; $n_1 = \rho_1/m_p = 1 \text{ cm}^{-3}$. The solid (blue) curves are calculated using the mechanical model (see Section 4). The dotted (red) curves show, for comparison, the solution of Figure 3 (found for the pressure balance). Two sets of solutions differ significantly; in particular, the blast wave found for the mechanical model decelerates slower and propagates farther (Panel c) until the RS arrives at the same last shell ($\tau = 50 \text{ s}$) in the ejecta (Panel a). The solid curves satisfy the energy-conservation law for the adiabatic blast wave; see Figure 6.

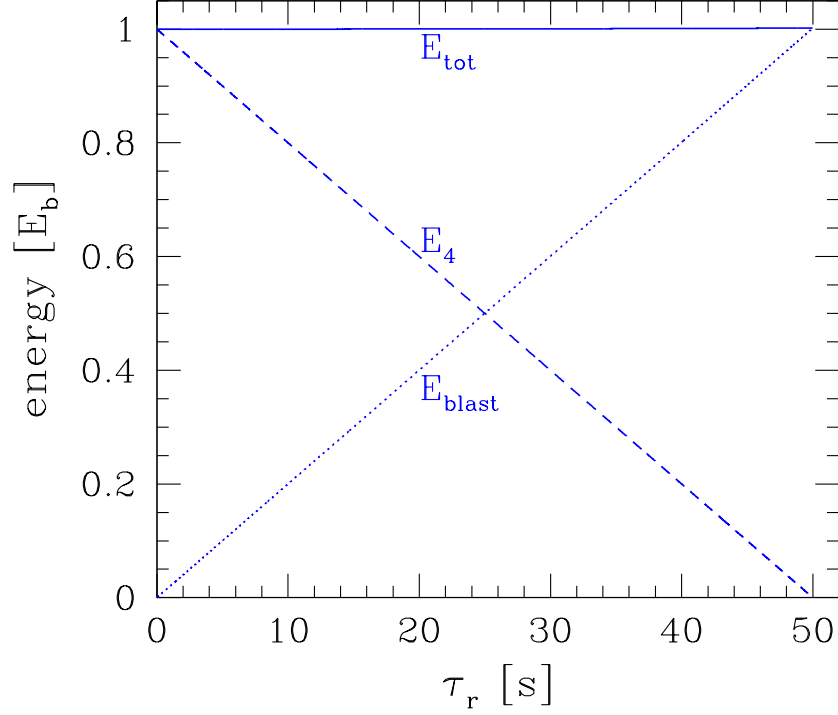


Fig. 6.— The energy E_{blast} of the blast (dotted line), the energy E_4 of region 4 (dashed line), and the total energy E_{tot} of the entire system (solid line; $E_{\text{tot}} = E_{\text{blast}} + E_4$) for the blast-wave evolution shown in Figure 5 (i.e., the solid blue curves found for the mechanical model). The energy E_b is the same as in Figure 4. The energies E_{blast} , E_4 , and E_{tot} are shown in the units of E_b for the τ_r -shell, i.e., the location of the RS in the ejecta. The blast energy E_{blast} here is found as in the equation (93) for the mechanical model. The total energy is precisely conserved above; thus the mechanical model successfully resolves the energy-violation problem seen in Figure 4.

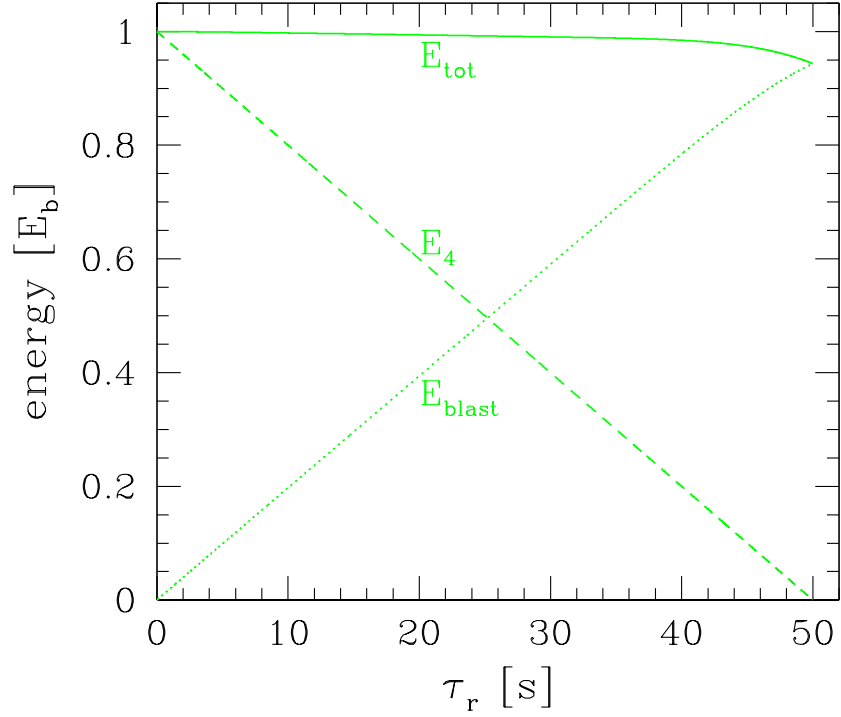


Fig. 7.— The same as in Figure 6, except for an alternative method of finding the blast energy E_{blast} . The blast energy here is found by evaluating the expression (64), while making use of an approximate pressure profile of a quadratic function for the blast (see Discussion; 4th paragraph). The total energy E_{tot} is conserved within about 5 % above; thus the quadratic pressure profile is a reasonably good approximation for the mechanical model.

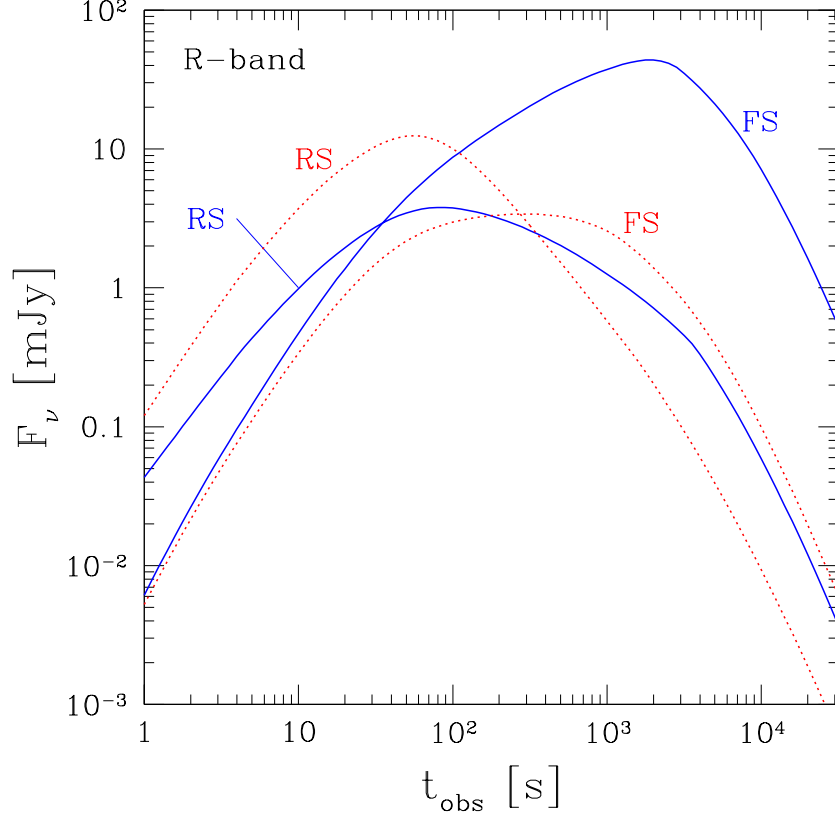


Fig. 8.— Afterglow light-curves in R-band, obtained for the same example burst as in Figure 5. FS and RS indicate the emissions from region 2 (FS-shocked) and 3 (RS-shocked), respectively. The solid (blue) curves are calculated using the mechanical model, corresponding to the solid (blue) curves in Figure 5. The dotted (red) curves are obtained using the pressure balance, corresponding to the dotted (red) curves in Figure 5. The emission parameters are $\epsilon_B = 0.01$, $\epsilon_e = 0.1$, and $p = 2.3$. The burst is assumed to be located at a cosmological redshift $z = 1$. The two different blast-wave evolutions shown in Figure 5 yield significantly different light-curves. The afterglow calculations are terminated when the RS arrives at the last shell ($\tau = 50$ s) in the ejecta. Thus, from $t_{\text{obs}} \sim \text{few} \times 10^3$ s, the light-curves are produced by high latitude emissions.

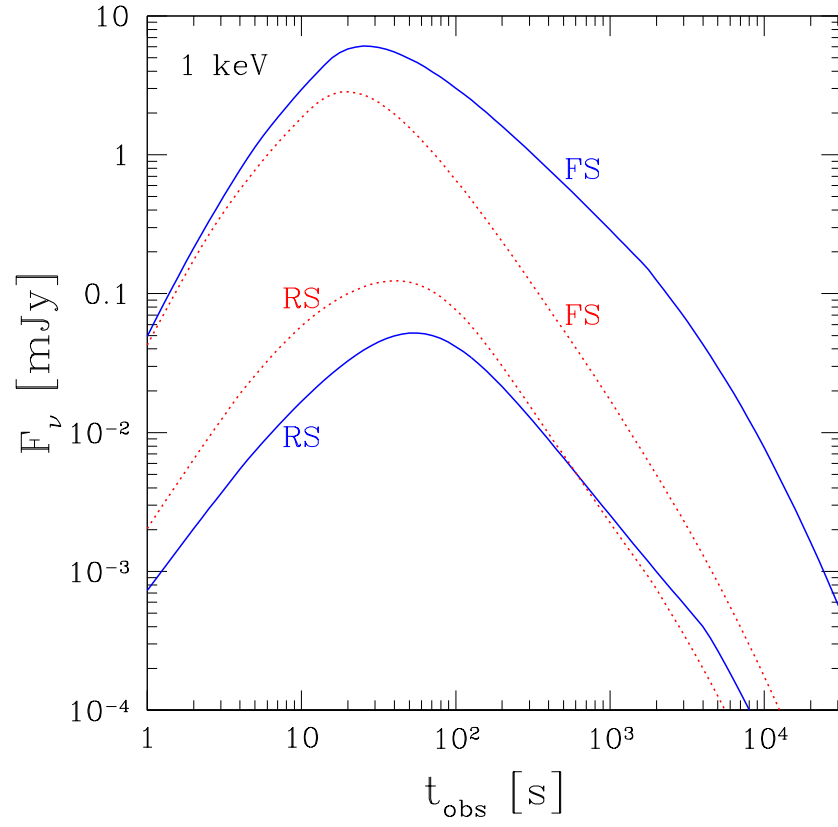


Fig. 9.— The same as in Figure 8, but in X-ray (1 keV) band.